Journal of Crystal Growth 385 (2014) 72–76

Contents lists available at ScienceDirect

Journal of Crystal Growth

journal homepage: www.elsevier.com/locate/jcrysgro

Combined effect of crucible rotation and magnetic field on hydrothermal wave

Y. Takagi [a,*], Y. Okano [a], H. Minakuchi [b], S. Dost [c]

[a] Department of Materials Engineering Science, Osaka University, 1-3 Machikaneyama, Toyonaka, Osaka 560-8531, Japan
[b] Department of Mechanical Systems Engineering, University of the Ryukyus, 1 Senbaru, Nishihara, Okinawa 903-0213, Japan
[c] Crystal Growth Laboratory, University of Victoria, Victoria, BC, Canada V8W 3P6

ARTICLE INFO

Available online 19 June 2013

Keywords:
A1. Computer simulation
A1. Convection
A1. Fluid flow
A1. Magnetic fields

ABSTRACT

The combined effect of crucible rotation and applied magnetic field on hydrothermal wave was investigated through a three-dimensional simulation. The computational domain was a shallow annular pool filled with a silicon melt, subjected to a crucible rotation and a vertical static magnetic field. The thermocapillary flow along the free surface was considered. Governing equations of the system were solved numerically by the finite volume method. The efficiency of controlling hydrothermal wave with crucible rotation and magnetic field was assessed. Results showed that although the hydrothermal wave was completely suppressed under the effect of magnetic field alone, the optimum combination of the body forces induced by the applied crucible rotation and magnetic field provides a better control of the hydrothermal wave.

1. Introduction

Hydrothermal wave (HTW) is the propagation phenomenon of temperature and velocity fluctuations observed along the free surface of a liquid. HTW develops due to the thermocapillary convective flow induced by the surface tension gradient in the liquid along the free surface. The strength of this thermocapillary flow is described by the dimensionless Marangoni number. This flow in the liquid is two-dimensional and stable at low Marangoni number values, however, the flow becomes three-dimensional and unstable as the Marangoni number increases.

The critical condition at which a HTW develops was theoretically investigated by Smith and Davis [1,2]. The development of a HTW is clearly seen in a shallow liquid pool during the final stage of Czochralski crystal growth [3]. The HTW analysis is free from the influence of the effect of natural convection. Thus, this makes the HTW analysis very useful in investigating the relative contribution of Marangoni convection. From these points of view, the dynamics and instability of HTW in a shallow annular pool were investigated numerically in Refs. [4–9]. In these studies, the control of HTW was not fully examined, and only the effect of pool (crucible) rotation was taken into account [5]. In the present study, we have examined numerically the combined effect of applied magnetic field and crucible rotation, and introduced an effective method to control HTW.

* Corresponding author. Tel./fax: +81 6 6850 5849.
E-mail address: takagi@cheng.es.osaka-u.ac.jp (Y. Takagi).

0022-0248/$ - see front matter © 2013 Elsevier B.V. All rights reserved.
http://dx.doi.org/10.1016/j.jcrysgro.2013.04.062

2. Numerical method

A schematic view of the computational domain is shown in Fig. 1. The silicon melt is contained in a shallow annular pool of depth $d=3$ mm, inner radius $r_i=15$ mm and outer radius $r_o=50$ mm. The upper boundary is a free surface and other boundaries are solid wall. The pool rotates with an angular velocity ω around the z-axis, and an applied magnetic field in the same direction. It was assumed that the silicon melt is an incompressible, Newtonian fluid, and the Boussinesq approximation holds. Under these assumptions, the governing equations of the liquid phase (silicon melt) take the following forms:

Continuity:

$$\nabla \cdot \mathbf{v} = 0 \tag{1}$$

Momentum:

$$\frac{\partial \mathbf{v}}{\partial t} + (\mathbf{v} \cdot \nabla)\mathbf{v} = -\frac{1}{\rho}\nabla p + \nu \nabla^2 \mathbf{v} + \beta g (T - T_C)\mathbf{e}_z + \mathbf{F}_M \tag{2}$$

Energy:

$$\frac{\partial T}{\partial t} + (\mathbf{v} \cdot \nabla) T = \alpha \nabla^2 T \tag{3}$$

Magnetic field:

$$\frac{\partial \mathbf{B}}{\partial t} - \nabla \times (\mathbf{v} \times \mathbf{B}) = \frac{1}{\mu_0 \sigma} \nabla^2 \mathbf{B} \tag{4}$$

where $\mathbf{v}$ is the flow velocity vector, t time, ρ the melt density, p pressure, β the thermal expansion coefficient, g the gravitational constant, T temperature, T_C temperature of the inner wall, $\mathbf{e}_z$ the

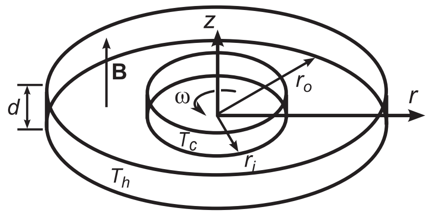

Fig. 1. Schematics of the computational domain.

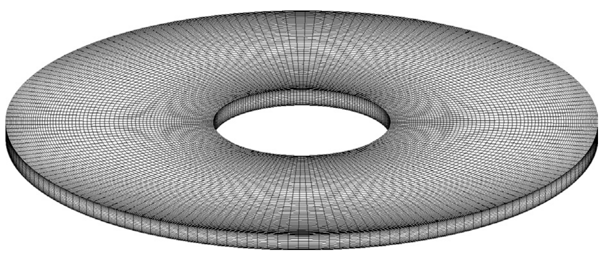

Fig. 2. Computational grid of the HTW simulation.

unit vector along the z-axis, $\mathbf{F}_M$ the Lorentz force induced by the magnetic applied field, α the melt thermal diffusivity, $\mathbf{B}$ magnetic flux, μ_0 magnetic permeability, and σ electric conductivity.

Eq. (4) is the magnetic field equation derived from the well-known Maxwell's equations [10]. The Lorentz force in Eq. (2) is calculated by

$$\mathbf{F}_M = \mathbf{J} \times \mathbf{B} = \frac{1}{\mu_0}(\nabla \times \mathbf{B}) \times \mathbf{B} \tag{5}$$

where $\mathbf{J}$ is the induced electric current.

The governing equations of the system (Eqs. (1)–(4)) were discretized by the finite volume method, and were solved by the PISO algorithm. Computations were carried out by using the OpenFOAM code. We assume no slip boundary conditions for the flow velocity field on the solid boundary, which determines the circumferential flow velocity on the boundary from the angular velocity of the pool rotation. Along the free surface, the induced flow velocity (by the Marangoni convection) was related to temperature gradient as follows:

$$\mu \frac{\partial \mathbf{v}}{\partial \mathbf{n}} = \gamma_T \nabla T \tag{6}$$

where $\mathbf{n}$ is the unit normal to the free surface. The computational grid shown in Fig. 2 was made in a cylindrical coordinate system and the grid points were clustered near the solid wall and the free surface. The grid numbers in the radial – (r), circumferential – (θ), and vertical – (z) directions are 81, 180 and 21, respectively. The maximum values of the dimensionless wall distance y^+ (normalized coordinate with respect to kinematic viscosity and friction velocity) on the inner, outer and bottom walls were 3.64, 1.16 and 1.06, respectively. These grid resolutions near the wall were sufficient to capture the boundary layer, therefore, a turbulence model was not adopted.

Physical properties of the silicon melt are listed in Table 1. The Prandtl number of the silicon melt is 1.09×10^{-2}. Other numerical parameters and the dimensionless numbers involved (the Marangoni number $Ma = -\gamma_T \Delta T (r_o - r_i)/\mu\alpha$, the Grashof number $Gr = g\beta\Delta T d^3/\nu^3$, the rotation Reynolds number $Re_\omega = r_o^2\omega/\nu$ and the Hartmann number $Ha = B_0(r_o - r_i)(\sigma/\nu)^{1/2}$) are presented in Table 2. The relative strength of natural convection with respect to the Marangoni convection, which is estimated with the ratio of Grashof and Marangoni numbers $Gr^{1/2}/Ma^{2/3}$ [11] is small: 2.70×10^{-4}. Thus, the contribution of the gravitational term $\beta g(T - T_C)\mathbf{e}_z$ in Eq. (2) was neglected in the present numerical simulation. This condition of neglecting the gravitational effect is valid for very shallow pools.

Table 1
Physical properties of silicon melt [4,12].

Property	Symbol	Value
Thermal conductivity (W m^{-1} K^{-1})	λ	64
Viscosity (kg m^{-1} s^{-1})	μ	7.0×10^{-4}
Density (kg m^{-3})	ρ	2530
Gravitational acceleration (m s^{-2})	g	9.81
Thermal expansion coefficient (K^{-1})	β	1.5×10^{-4}
Surface tension coefficient (Nm^{-1} K^{-1})	γ_T	-7.0×10^{-5}
Heat capacity (J kg^{-1} K^{-1})	C_p	1000
Melting temperature (K)	T_m	1683
Electric conductivity (Sm^{-1})	σ	1.2×10^6
Magnetic permeability (Hm^{-1})	μ_0	1.26×10^{-6}

Table 2
Numerical parameters of the HTW simulation.

Parameter	Symbol	Value
Innner wall temperature (K)	T_c	1683
Temperature diffrence (K)	ΔT	21
Marangoni number (–)	Ma	2.91×10^3
Grashof number (–)	Gr	3.01×10^{-3}
Rotation speed (min^{-1})	ω	0, 1, 2, 5
Rotating Reynolds number (–)	Re_ω	0, 946, 1892, 4731
Magnetic flux density (mT)	B_0	0, 26.3, 39.5, 52.6
Hartmann number (–)	Ha	0, 38, 57, 72

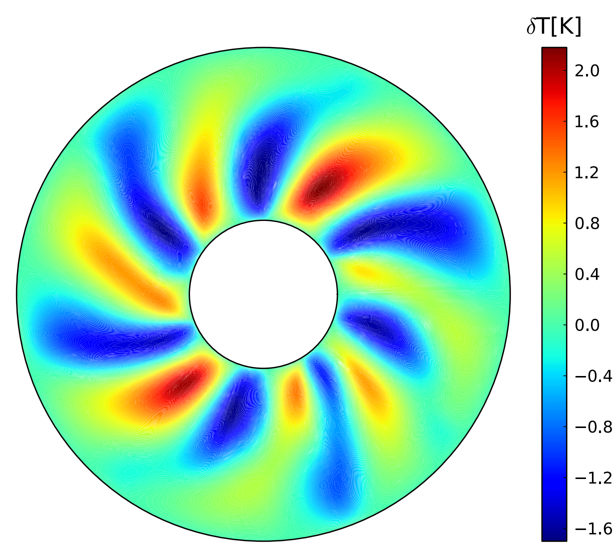

Fig. 3. Surface temperature fluctuation without external force at $t = 150$ s.

3. Results and discussion

3.1. Validation of the simulation code

Before the actual simulations, we have first validated the simulation code in the absence of external body forces (induced by the applied crucible rotation and magnetic field). The simulation results of the validation are presented in Figs. 3–5.